雑誌

発表者氏名	論文タイトル名	発表誌名	巻号	ページ	出版年
Utoh R, Tateno C, Kataoka M, Tachibana A, Masumoto N, Yamasaki C, Shimada T, Itamoto T, Asahara T, Yoshizato K.	Hepatic Hyperplasia Associated with Discordant Xenogeneic Parenchymal-Nonparenchymal Interactions in Human Hepatocyte-Repopulated Mice.	American Journal of Pathology	177	654-665	2010
Kikuchi R, McCown M, Olson P, Tateno C, Morikawa Y, Kato Y, Bourdet D, Monshouwer M, and Fretland AJ.	Effect of HCV infection on the mRNA expression of drug transporters and cytochrome P450 enzymes in chimeric mice with humanized liver	Drug Metabolism and Disposition	38	1954-1961	2010
Yamasaki C, Kataoka M, Kato Y, Kakuni M, Usuda S, Ohzone Y, Matsuda S, Adachi Y, Ninomiya S, Itamoto T, Asahara T, Yoshizato K, and Tateno C.	In Vitro Evaluation of Cytochrome P450 and Glucuronidation Activities in Hepatocytes Isolated from Liver-Humanized Mice.	Drug Metabolism and Pharmacokinetics	25	539-550	2010

寺岡弘文

書籍　なし

著者氏名	論文タイトル名	書籍全体の編集者名	書　籍　名	出版社名	出版地	出版年	ページ

雑誌

発表者氏名	論文タイトル名	発表誌名	巻号	ページ	出版年
Masaki H, et al.	DPPA4 modulates chromatin structure via association with core histone H3 and DNA in mouse embryonic stem cells	Genes to Cells	15(4)	327-337	2010

Sakasai R, et al.	Transcription-dependent activation of ataxia telangiectasia- mutated prevents DNA-dependent protein kinase-mediated cell death in response to topoisomerase I	Journal of Biological Chemistry	285(20)	15201-15208	2010

田中靖人

書籍　なし

著者氏名	論文タイトル名	書籍全体の編集者名	書　籍　名	出版社名	出版地	出版年	ページ

雑誌

発表者氏名	論文タイトル名	発表誌名	巻号	ページ	出版年
Wu S, Imazeki F, Kurbanov F, Fukai K, Arai M, Kanda T, Yonemitsu Y, **Tanaka Y**, Mizokami M, Yokosuka O.	Evolution of hepatitis B genotype C viral quasi-species during hepatitis B e antigen seroconversion.	J Hepatol.	54(1)	19-25	2011
Yokosuka O, Kurosaki M, Imazeki F, Arase Y, **Tanaka Y**, Chayama K, Tanaka E, Kumada H, Izumi N, Mizokami M, Kudo M.	Management of hepatitis B: Consensus of the Japan Society of Hepatology 2009.	Hepatol Res.	41(1)	1-21	2011
Yuen MF, Ka-Ho Wong D, Lee CK, **Tanaka Y**, Allain JP, Fung J, Leung J, Lin CK, Sugiyama M, Sugauchi F, Mizokami M, Lai CL.	Transmissibility of Hepatitis B Virus (HBV) Infection through Blood Transfusion from Blood Donors with Occult HBV Infection.	Clin Infect Dis.	52(5)	624-32	2011

中西真

書籍　なし

著者氏名	論文タイトル名	書籍全体の編集者名	書　籍　名	出版社名	出版地	出版年	ページ

雑誌

発表者名	論文タイトル名	発表誌名	巻号	ページ	出版年
Shimada, M., Haruta, M., Niida, H., Sawamoto, K., and *Nakanishi, M.	PP1g is a phosphatase responsible for dephosphorylation of histone H3 at threonine 11 after DNA damage.	***EMBO rep.***	11	883-889	2010
Niida, H., Murata, K., Shimada, M., Ogawa, K., Ohta, K., Suzuki, K., Fujigaki, H., Khaw, A.K., Banerjee, B., Hande, P.M., Miyamoto, T., Miyoshi, I., Shirai, T., Motoyama, N., Delhase, M., Appella, E., and *Nakanishi, M.	Cooperative functions of Chk1 and Chk2 reduce tumor susceptibility in vivo.for Chronic Hepatitis C.	***EMBO J.***	29	3558-3570	2010
Niida, H., Katsuno, Y., Sengoku, M., Shimada, M., Yukawa, M., Ikura, M., Ikura, T., Kohno, K., Shima, H., Suzuki, H., Tashiro, S., and *Nakanishi, M.	Essential role of Tip60-dependent recruitment of ribonucleotide reductase at DNA damage sites in DNA repair during G1 phase.	***Genes and Dev.***	24	333-338	2010

水口裕之

書籍

著者氏名	論文タイトル名	書籍全体の編集者名	書　籍　名	出版社名	出版地	出版年	ページ
川端健二，田代克久，水口裕之．	iPS 細胞への遺伝子導入を用いた分化誘導の最適化		*薬学雑誌*	日本薬学会	日本	2010	1527-1534

雑誌

発表者氏名	論文タイトル名	発表誌名	巻号	ページ	出版年
Inamura M, Kawabata K, Takayama K, Tashiro K, Sakurai F, Katayama K, Toyoda M, Akutsu H, Miyagawa Y, Okita H, Kiyokawa N, Umezawa A, Hayakawa T, Furue MK, Mizuguchi H.	Efficient generation of hepatoblasts from human ES cells and iPS cells by transient overexpression of homeobox gene HEX.	*Mol. Ther.*,	19	400-7	2011

Hepatology Research

Hepatology Research 2011; 41: 375–385 doi: 10.1111/j.1872-034X.2010.00769.x

Original Article

Pitavastatin inhibits hepatic steatosis and fibrosis in non-alcoholic steatohepatitis model rats

Tomokatsu Miyaki,[1] Shunsuke Nojiri,[1] Noboru Shinkai,[1] Atsunori Kusakabe,[1] Kentaro Matsuura,[1] Etsuko Iio,[1] Satoru Takahashi,[2] Ge Yan,[3] Kazuo Ikeda[3] and Takashi Joh[1]

Departments of [1]Gastroenterology and Metabolism, [2]Experimental Pathology and Tumor Biology, and [3]Cell Biology and Anatomy, Nagoya City University Graduate School of Medical Sciences, Nagoya, Aichi, Japan

Aim: Non-alcoholic steatohepatitis (NASH) may progress to liver cirrhosis, and NASH patients with liver cirrhosis are at risk of developing hepatocellular carcinoma. Statins, 3-hydroxy-3-methyglutaryl-coenzyme A reductase inhibitors, are well known to reduce low-density lipoprotein cholesterol and reduce the incidence of coronary heart disease and other major vascular events by anti-inflammatory and antifibrotic effects, and antiproliferative properties in colorectal cancers have also been reported. Recently, statins have been reported to improve hepatic steatosis; however, the effect on fibrosis is controversial.

Methods: The effects of pitavastatin (one of the strongest statins) were examined using a choline-deficient L-amino acid-defined (CDAA) diet liver fibrosis model.

Results: Pitavastatin significantly attenuated increases in serum aspartate aminotransferase, alanine aminotransferase, hepatic steatosis, oxidative stress, pre-neoplastic lesions (glutathione S-transferase placental form-positive lesions), expression of cytokines, such as tumor necrosis factor-α and transforming growth factor-β1, and the expression of tissue inhibitor of metalloproteinase-1, tissue inhibitor of metalloproteinase-2 and type I procollagen genes followed by attenuating fibrosis of the liver of CDAA-fed rats.

Conclusion: These results indicate that pitavastatin may inhibit steatosis, hepatic fibrosis and carcinogenesis in rat model of NASH.

Key words: NASH, statin, steatosis, fibrosis

INTRODUCTION

NON-ALCOHOLIC STEATOHEPATITIS (NASH) is a common liver disease that may progress to cirrhosis, liver failure and liver cancer. The histological findings of NASH are characterized by steatosis, hepatic inflammation and injury to liver cells. In patients with highly progressive fibrosis in NASH, the 5-year cumulative incidence of hepatocellular carcinoma (HCC) was 20%[1] and HCC seemed to occur in advanced fibrotic stages in the liver, but the natural history of NASH has not yet been revealed.

Various factors are involved in the transition from non-alcoholic fatty liver disease (NAFLD) to NASH. The two-hit theory postulating the existence of an additional factor (second hit) after steatosis (first hit) has been generally proposed,[2,3] and oxidative stress and insulin resistance in its background are considered to be important. Because the causes of NASH are diverse, no definite therapy has been established. Recently, several reports have revealed the improvement of NASH, such as by the antioxidant vitamin E (α-tocopherol),[4] angiotensin II type 1 receptor blocker (ARB),[5,6] insulin resistance-improving agents[7] and peroxisome proliferator-activated receptor (PPAR)-γ ligand in NASH patients[8] and NASH model rats.[9] On the other hand, some controversial papers have been reported.[10]

Statins, 3-hydroxy-3-methyglutaryl-coenzyme A (HMG-CoA) reductase inhibitors, are well known to reduce low-density lipoprotein (LDL) cholesterol concentrations and to reduce the incidence of coronary heart disease and other major vascular events.[11] Some experimental reports have revealed that statins can reduce liver triglyceride[12] and ameliorate severe hepatic steatosis,[13] and are therefore capable of improving NASH. On the other hand, clinically, the study of statin treatment for NASH is not adequate.[14–16] It has been

Correspondence: Dr Shunsuke Nojiri, Department of Gastroenterology and Metabolism, Nagoya City University Graduate School of Medical Sciences, 1 Kawasumi, Mizuho-cho, Mizuho-ku, Nagoya, Aichi 467-8601, Japan. Email: snojiri@med.nagoya-cu.ac.jp
Received 9 April 2010; revised 27 November 2010; accepted 18 December 2010.

reported that statins improved liver steatosis or the non-alcoholic fatty liver disease activity score but their efficacy for fibrosis is controversial. It is well known that statins have many non-cholesterol-dependent effects as well as cholesterol-lowering effects[17] and some antifibrotic effects have been reported.[18] We therefore hypothesized that statins had inhibiting effects not only on triacylglycerol (TG) consumption and inflammation but also on fibrogenesis and carcinogenesis of the liver. A study of the effects on statins on all these effects in NASH has not been reported. The aim of this study was to investigate the experimental inhibiting effects on steatosis, fibrosis and carcinogenesis of statins in NASH using a rat model and to reveal the clinically useful potential of statins for NASH.

METHODS

Animals

SIX-WEEK-OLD male Wistar rats were purchased from CLEA Japan Inc. (Tokyo, Japan), housed under controlled lighting (12:12-h light : dark cycle), and food and water were freely accessible throughout the study period. Pitavastatin was purchased from Kowa Pharmaceutical (Tokyo, Japan). The choline-deficient L-amino acid-defined (CDAA) diet and choline-supplemented L-amino acid-defined (CSAA) diet were obtained in powder form (Dyets, Bethlehem, PA, USA), as described in previous reports.[19,20] Pitavastatin powder was mixed uniformly into the CDAA and CSAA diets at concentrations of 0 and 5 (mg/kg per day). Based on the national regulations and guidelines, all experimental procedures were reviewed by the Institutional Laboratory Animal Care and Use Committee (IACUC) of Nagoya City University, and were finally approved by the President of the University (no. H19-04).

Experimental protocol

The study periods were 2 and 10 weeks. In the 2-week experiment, two groups of eight rats each received a CSAA diet containing 0 and 5 mg/kg per day pitavastatin, and two groups of eight rats each received a CDAA diet containing 0 and 5 mg/kg per day pitavastatin. In the 10-week experiment, similarly, two groups of eight rats each received a CSAA diet or a CDAA diet containing 0 and 5 mg/kg per day pitavastatin. We measured the amount of food that the rats ate every day to determine the amount of pitavastatin necessary to establish a daily dose of 5 mg/kg of rat weight. As food consumption among the rats was essentially equally, we considered that 5 mg/kg per day pitavastatin was consumed during the experimental periods.

Biochemical parameters

In all experiments, serum aspartate aminotransferase (AST), alanine aminotransferase (ALT) and TG were measured.

Histopathological and immunohistochemical examinations

Five-micrometer-thick sections of the right lobe of all rat livers, fixed in 10% formalin for 24 h and embedded in paraffin, were processed for hematoxylin–eosin and Masson trichrome staining. Glutathione S-transferase placental form (GST-P)-positive lesions (as suitable markers for pre-neoplastic lesions in rat hepatocarcinogenesis)[21] and nitrotyrosine-positive lesions (as oxidant stress)[22] (#06–286 upstate) were immunohistochemically assessed employing the avidin–biotin–peroxidase complex method. Fat drops, fibrosis, nitrotyrosine and GST-P-positive areas in the liver were quantified using a Provis microscope (Olympus, Tokyo, Japan) equipped with a charge-coupled device camera (Sony, Tokyo, Japan), and subjected to computer-assisted analysis with IPAP-WIN software (Sumitomo Techino Service, Hyogo, Japan). Ten different randomly selected areas per specimen were analyzed. The areas of fat drops, fibrosis and nitrotyrosine-positive cells were expressed as a percentage of the total area of the specimen. GST-P-positive lesions were expressed as a percentage of the total area, and the number of GST-P-positive lesions was counted in 10 specimens.

Real-time polymerase chain reaction (PCR) for quantitative assessment of mRNA expression

Tissue inhibitor of metalloproteinase-1 (TIMP-1), tissue inhibitor of metalloproteinase-2 (TIMP-2), matrix metalloproteinase-2 (MMP-2) and tumor necrosis factor-α (TNF-α) have been implicated in fibrosis in NASH, and transforming growth factor-β1 (TGF-β1) is also a key cytokine causing fibrinogenesis in NASH. We therefore examined their expressions.

Total RNA was extracted using Trizol reagent according to the manufacturer's recommended protocol (Life Technologies, Grand Island, NY, USA). RNA extracts were reverse-transcribed with random hexamers and avian myeloblastosis virus reverse transcriptase using a commercial kit (Takara, Kyoto, Japan). Expressions of TIMP-1, TIMP-2, MMP-2, TNF-α, and type I procollagen were evaluated by real-time PCR using an ABI

prism 7000 Sequence Detection system (Applied Biosystems, Tokyo, Japan) according to the manufacturer's protocol. Probes and primers for TIMP-1 (ID: Rn00587558_m1), TIMP-2 (ID: Rn00573232_m1), MMP-2 (ID: Rn02532334_s1), TNF-α (ID: Rn99999017_m1), type I procollagen α1 (ID: Rn00901649_g1) and TGF-β1 (ID: Rn00572010_A1) were purchased from Applied Biosystems. The relative target was glyceraldehyde-2-phosphate dehydrogenase (GAPDH; ID: 4352338E) mRNA in an identical cDNA sample using the standard curve method recommended by the manufacturer.

Western blot analysis

For the analysis of protein expression, liver specimens were disrupted in lysis buffer containing (final concentrations) 25 mmol/L HEPES (pH 7.4), 120 mmol/L NaCl, 5 mmol/L ethylene glycol tetraacetic acid, 10% glycerol, 1% Triton X-100, 50 mmol/L NaF, 100 μM Na-o-vanadate, 5 mmol/L Na-pyrophosphate and protease inhibitor cocktail. After 10 min on ice, lysates were centrifuged on ice for 5 min and either used immediately or stored at −70°C until use. The lysates were dissolved in Laemmli buffer, and then placed in a bath of boiling water for 5 min. Subsequently, each sample was separated by 10% sodium dodecylsulfate polyacrylamide gel electrophoresis and transferred to polyvinylidene fluoride membranes. After blocking with 1% bovine serum albumin in Tris-buffered saline Tween-20 (TBST) (20 mmol/L Tris [pH 8.0], 150 mmol/L NaCl and 0.01% Triton X-100) for 1 h at room temperature, the samples were probed with anti-TGF-β1 (IC.5559-100; Biovision Inc., San Francisco, CA, USA), anti-α-smooth muscle actin (α-SMA) antibody (Dako Japan, Tokyo, Japan), and anti-PPAR-γ antibody (sc-7196 rabbit polyclonal antibody), followed by goat anti-mouse or antirabbit antibody conjugated with horseradish peroxidase. After extensive washing with TBST, membranes were treated with enhanced chemiluminescence reagent (Amersham Pharmacia Biotech Inc., Schenctady, NY, USA). Bands were quantified densitometrically. Where required, the density of each band was normalized by comparison to the β-actin (using ab6276-100 antibody; ABcam, Cambridge, MA, USA) protein bands measured in the same membrane.

Serum TGF-β1 concentration determined by enzyme-linked immunosorbent assay and quantification of TG in liver

The TGF-β1 concentration in serum was measured using an Immunoassay Kit (KAC1688; BioSource). TG was measured using a Triglyceride Quantification Kit (Bio-Vision) according to the instructions.

Human hepatic stellate cell line LX-2

Human hepatic stellate cell line LX-2, which was kindly donated by Dr Scott L Friedman, was used to analyze pitavastatin efficacy for the inactivation of human hepatic stellate cells (HSC).[23] The LX-2 cell line was cultured in Dulbecco's modified Eagle's medium (DMEM) (Nissui Pharmaceutical, Tokyo, Japan) with 10% fetal bovine serum. Cells were seeded at a density of 5.0×10^5 cell/mL in monolayer culture on uncoated 60-mm plastic dishes. All cultures were incubated at 37°C in a humidified atmosphere of 5% air. Medium with or without pitavastatin was changed and, after 24 h, the culture cells were harvested with lysis buffer.

Isolation and culture of HSC and culture HSC

Rat HSC were isolated as described previously with some modifications.[24] In brief, the liver was perfused *in situ* via the portal vein with Ca^{2+}, Mg^{2+}-free Krebs–Ringer (KR) solution followed by 0.1% pronase E (Merck, Darmastadt, Germany) and then 0.032% collagenase (Wako Pure Chemicals, Osaka, Japan) solution at 37°C. The digested liver was minced, and incubated in KR solution containing 0.08% pronase E, 0.04% collagenase and 20 μg/mL DNase (Boehringer-Mannheim, Mannheim, Germany) for 30 min at 37°C (pH 7.3). The resulting suspension was then passed through a nylon mesh. The filtrate was centrifuged at 450 *g* for 8 min. A fraction enriched with HSC was finally obtained by centrifugation in 8.2% Nycodenz (Nycomed Pharma, Oslo, Norway) solution at 1400 *g* for 20 min at 4°C. HSC in the upper white layer were washed by centrifugation at 450 *g* for 8 min, suspended in DMEM containing 10% fetal calf serum (Commonwealth Serum Laboratories, Melbourne, Australia), and supplemented with 100 U/mL penicillin and 100 mU/mL streptomycin (Gibco Laboratories, Life Technologies, Grand Island, NY, USA). Seeding conditions were the same as for cell line LX-2. After incubation for 4 h, non-adherent cells were removed with a pipette and the culture medium was replaced with medium containing pitavastatin or the same concentration of dimethylsulfoxide as a control. Medium with or without pitavastatin was changed every 24 h and cell culture was continued up to 3 days.

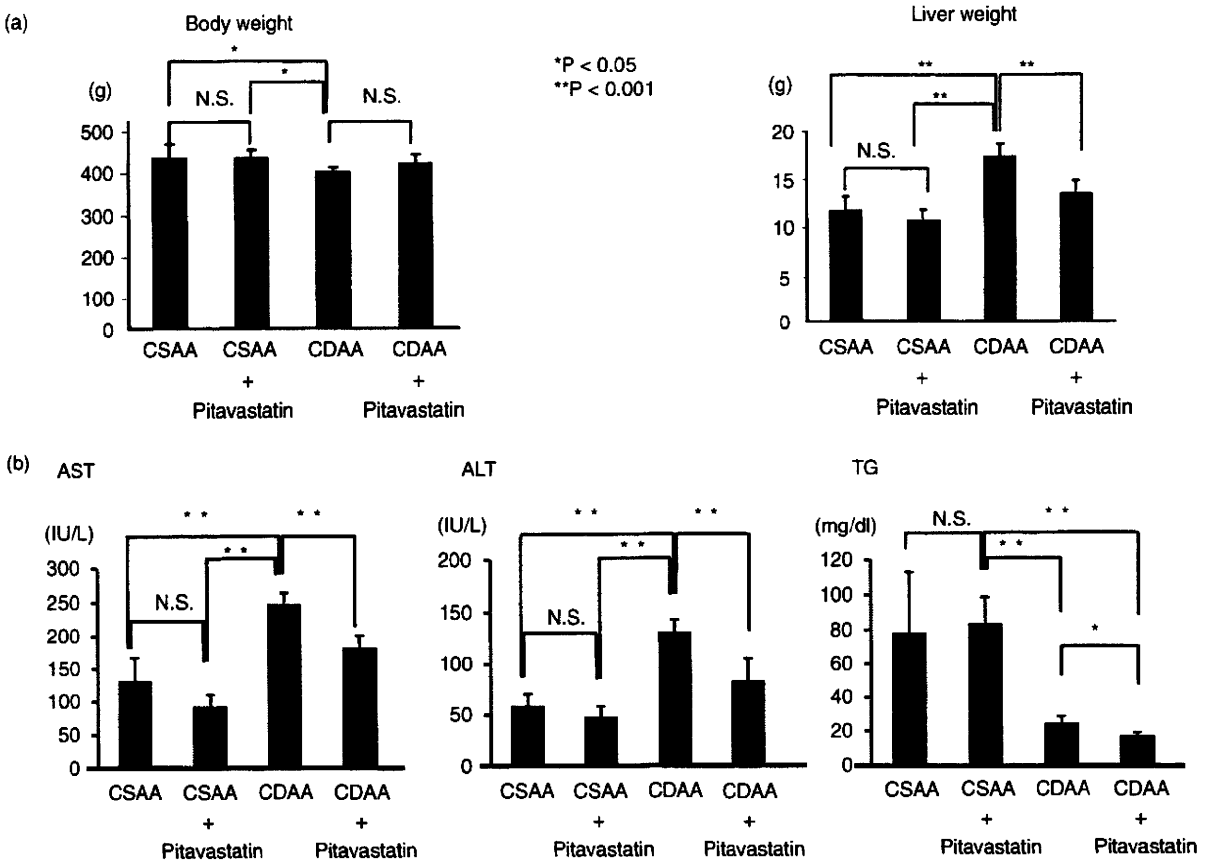

Figure 1 (a) Effect of pitavastatin on the characteristics of rats (10 weeks). Pitavastatin administration did not affect bodyweight changes in choline-supplemented L-amino acid-defined (CSAA)- or choline-deficient L-amino acid-defined (CDAA)-fed rats. The liver weight of CDAA-fed rats significantly increased compared to CSAA-fed rats. The administration of pitavastatin significantly attenuated the liver weight in CDAA-fed rats. (b) Effect of pitavastatin on serum markers (10 weeks). In CDAA-fed rats, aspartate aminotransferase (AST) and alanine aminotransferase (ALT) increased significantly, whereas pitavastatin reduced them. Triacylglycerol (TG) decreased in CDAA-fed rats, and pitavastatin more significantly reduced the level in this model. N.S., not significant.

Statistical methods

Statistical analysis was conducted using ANOVA. The results are expressed as the means ± standard deviation of four or more individual experiments.

RESULTS

Effect of pitavastatin on characteristics of rats

AFTER 10 WEEKS of feeding, the bodyweight of rats fed the CDAA diet was lower than those fed the CSAA diet, and pitavastatin had no influence on bodyweight, whereas rats fed the CDAA diet for 10 weeks showed an increase in the liver weight of 18.5 ± 2.1 g compared with 11.0 ± 0.9 g for rats fed the CSAA diet. Pitavastatin treatment at 5 mg/kg per day in CDAA-fed rats attenuated the increase in liver weight relative to that in CDAA-fed rats that did not receive pitavastatin ($P < 0.001$, Fig. 1a). The serum AST and ALT levels in CDAA-fed rats were significantly higher than in CSAA-fed rats; however, TG was lower in CDAA-fed than in CSAA-fed rats. Treatment of the CDAA-fed rats with pitavastatin decreased both AST and ALT levels (Fig. 1b).

Histological findings of liver steatosis

In this model, after 2 weeks, significant steatosis was observed in CDAA-fed rats, and pitavastatin attenuated

Table 1 Quantitative analysis of liver steatosis in choline-supplemented L-amino acid-defined (CSAA) or choline-deficient L-amino acid-defined (CDAA)-fed rats with or without pitavastatin

Treatment (no. of rats)	After 2 weeks		After 10 weeks	
Fat drop area (mean ± SD) (%)				
CSAA (8)	0	$P < 0.001$	0	$P < 0.001$
CDAA (8)	47.1 ± 5.8		30.7 ± 6.4	
CDAA + pitavastatin (8)	36.8 ± 3.7	$P < 0.001$	20.6 ± 5.0	$P < 0.05$
Quantitative triacylglycerol in the liver of CSAA- or CDAA-fed rats mg/g wet weight (mean ± SD)				
CSAA (8)	2.5 ± 1.9	$P < 0.001$	6.4 ± 2.9	$P < 0.001$
CDAA (8)	557.0 ± 73		201.5 ± 37.8	
CDAA + pitavastatin (8)	420.7 ± 99	$P < 0.001$	144.2 ± 14.6	$P < 0.001$

After 2 and 10 weeks, liver steatosis had progressed in CDAA-fed rats, and pitavastatin (5 mg/kg per day) decreased the development of liver steatosis.
After 2 and 10 weeks, triacylglycerol in the liver tissue had increased significantly in CDAA-fed rats and pitavastatin (5 mg/kg per day) attenuated its accumulation.
SD, standard deviation.

the development of steatosis, and the size of fat drops in hepatocytes of rats fed the CDAA diet with pitavastatin seemed to be smaller than in rats fed the CDAA diet without pitavastatin (data not shown). After 10 weeks, the same tendency was observed but the area of steatosis was reduced due to being occupied by fibrosis, and a lower level of significance was observed between with and without pitavastatin in CDAA-fed rats (Table 1). After 2 and 10 weeks, TG in the liver tissue had increased significantly in CDAA-fed rats and pitavastatin (5 mg/kg per day) attenuated its accumulation (Table 1).

Histological findings of fibrosis

Histological analysis of the livers of CDAA-fed rats at 10 weeks revealed extensive fibrosis and the accumulation of extracellular matrix. In contrast, pitavastatin significantly inhibited the development of liver fibrosis (Fig. 2a) shown with 5 mg/kg per day administration. Image analysis showed that the extent of liver fibrosis in CDAA-fed rats treated with pitavastatin was significantly reduced (Fig. 2ca).

Effect of pitavastatin on oxidative stress and GST-positive lesions in the rat liver (10 weeks)

Nitrotyrosine, a marker of oxidative stress, in liver sections was investigated immunohistochemically. Nitrotyrosine-positive cells were more frequent in the liver sections of CDAA-fed rats, and pitavastatin administration markedly reduced nitrotyrosine-positive cells (Fig. 2b,cb). GST-P-positive lesions consisted mainly of these nodules. It has been reported that GST-P[21] is a suitable marker of pre-neoplastic lesions in rat hepatocarcinogenesis. The results of quantitative analysis were studied. The concomitant administration of 5 mg/kg per day pitavastatin significantly reduced the number and area of GST-P-positive lesions, compared with the livers of rats fed the CDAA diet without pitavastatin (Fig. 3).

Effect of pitavastatin on rat liver fibrogenesis

To investigate the effect of pitavastatin on fibrogenesis and fibrolysis in the rat liver, we assessed mRNA expressions of TIMP-1, TIMP-2, MMP-2 and type I procollagen employing real-time PCR after 10 weeks (Fig. 4). TIMP-1, TIMP-2, MMP-2 and type I procollagen mRNA in the liver significantly increased in CDAA-fed compared to CSAA-fed rats. The addition of 5 mg/kg per day pitavastatin to the CDAA diet significantly reduced the expressions of TIMP-1, TIMP-2, MMP-2 and type I procollagen mRNA in the liver, compared with those of rats fed the CDAA diet without pitavastatin. The addition of 5 mg/kg per day pitavastatin to the CSAA diet caused no changes compared to the CSAA diet without pitavastatin.

Effect of pitavastatin on TNF-α, TGF-β1 and α-SMA

The relative expression of TNF-α mRNA was higher in CDAA-fed than in CSAA-fed rats, and pitavastatin significantly attenuated the expression of TNF-α (Fig. 4).

Protein in the serum and mRNA in the liver of TGF-β1 were examined. The protein levels of TGF-β1

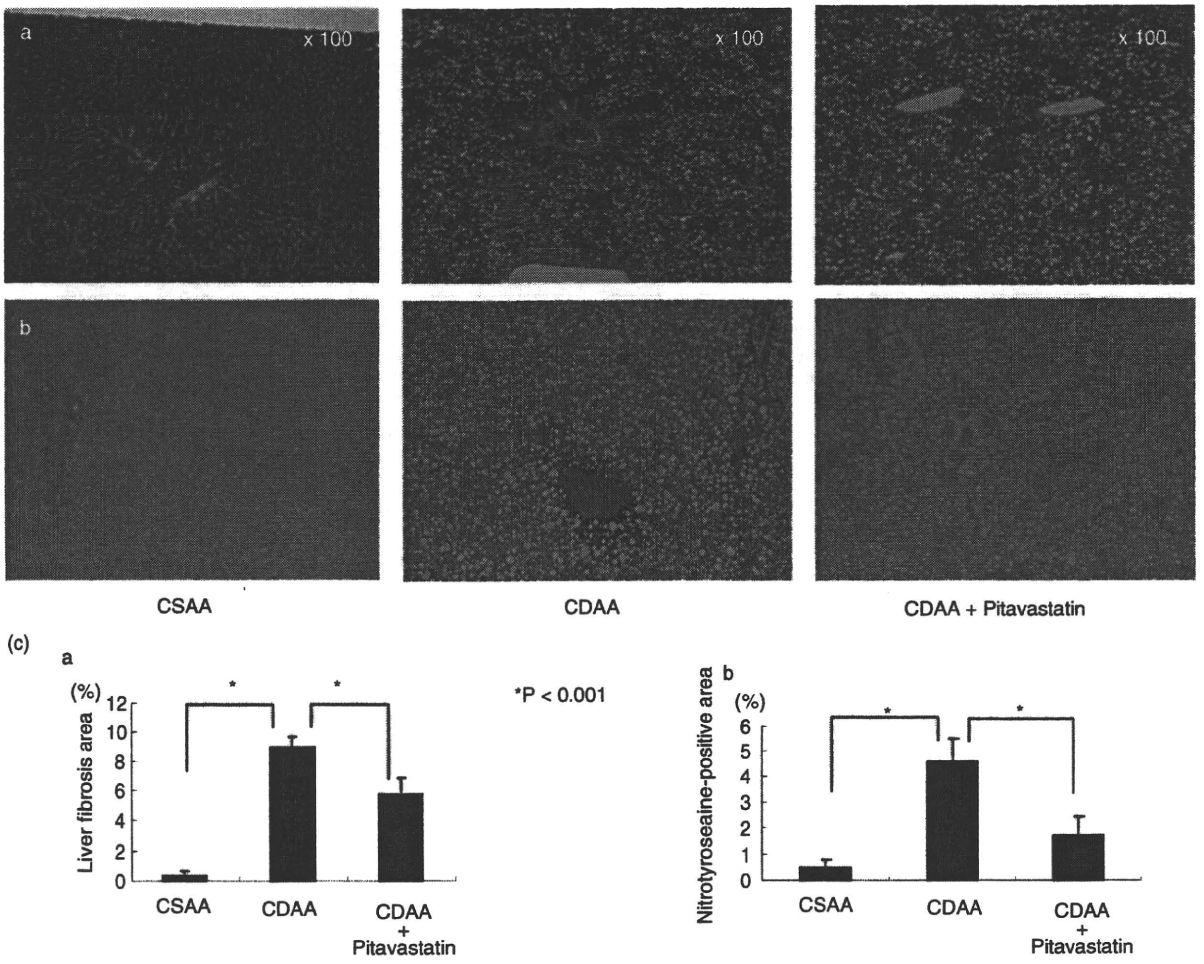

Figure 2 (a) Photomicrographs of liver sections stained with Masson trichrome staining. Choline-supplemented L-amino acid-defined (CSAA)-fed rat, choline-deficient L-amino acid-defined (CDAA)-fed rat and CDAA-fed rat with pitavastatin for 10 weeks. Pitavastatin markedly inhibited liver fibrosis (original magnification ×100). The degree of development of liver fibrosis was quantified using a computerized image analysis system. The liver fibrosis area is shown as a percentage of the microscopic field (ca). Liver histology of CDAA-fed rats showed severe fibrosis. The administration of pitavastatin significantly attenuated the development of fibrosis in CDAA-fed rats. Data are shown as the means ± standard deviations. (b) Photomicrographs of liver sections stained with nitrotyrosine in a CSAA-fed rat, CDAA-fed rat and CDAA-fed rat with pitavastatin for 10 weeks. Pitavastatin markedly inhibited oxidative stress (magnification ×100). The degree of oxidative stress in the liver was quantified using a computerized image analysis system (cb). Nitrotyrosine-positive cells in CDAA-fed rats increased significantly more than in CSAA-fed rats. The administration of pitavastatin significantly attenuated nitrotyrosine-positive cells in CDAA-fed rats. Data are shown as the means ± standard deviations.

in the serum of CDAA-fed rats were significantly higher than in CSAA-fed rats, and pitavastatin significantly attenuated its progression (Fig. 5a). The same effects were observed in the liver tissue. The mRNA expression of TGF-β1 for CDAA-fed rats was higher than that for CSAA-fed rats, and pitavastatin reduced the expression of TGF-β1 (Fig. 5b). As a marker of HSC activation, α-SMA expression was examined in the rat liver. In CDAA-fed rats, α-SMA expression was significantly higher than in CSAA-fed rats, and pitavastatin significantly attenuated its expression (Fig. 5c,d).

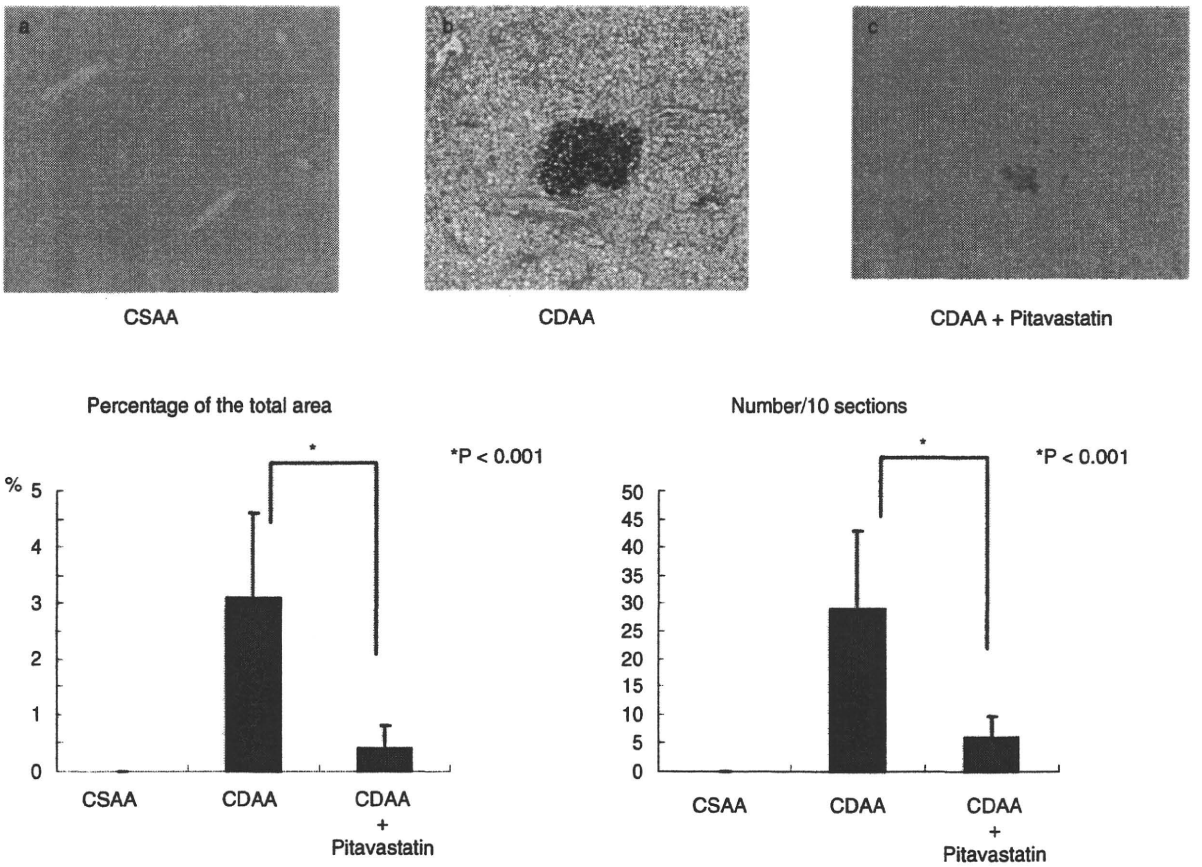

Figure 3 Photomicrographs of liver sections with stained glutathione S-transferase placental form (GST-P)-positive lesions in a choline-supplemented L-amino acid-defined (CSAA)-fed rat (a), choline-deficient L-amino acid-defined (CDAA)-fed rat (b) and CDAA-fed rat with pitavastatin (c) for 10 weeks (magnification ×100). The GST-P-positive percentage of the total area and numbers in 10 sections were measured and quantified using a computerized image analysis system. The GST-P-positive lesions in CDAA-fed rats increased, and the administration of pitavastatin significantly attenuated both the percentage of the total area and number in the 10 sections. Data are shown as the means ± standard deviations.

Effect of pitavastatin on the expression of α-SMA and PPAR-γ in HSC

To confirm the effect of pitavastatin on HSC, we measured the expression of α-SMA and PPAR-γ, an important inducer of TNF-α production, using human HSC lines (LX-2) (Fig. 6a) and isolated HSC from normal rats (Fig. 6b). α-SMA expression was decreased by adding pitavastatin dose-dependently and PPAR-γ expressions increased gradually in a dose-dependent manner. The same experiment was performed using freshly isolated HSC from normal rats. Three days after adding pitavastatin, α-SMA and PPAR-γ protein expressions were examined by western blotting. α-SMA decreased and PPAR-γ increased gradually by adding pitavastatin in a dose-dependent manner.

DISCUSSION

RECENTLY, VARIOUS CLINICAL statin treatments for NAFLD and NASH have been reported.[14–16,25–27] Almost all of these reports, except Nelson *et al.*,[27] describe the reduction of serum aminotransferase or reduction of steatosis of the liver. Nelson *et al.* reported that there was no statistically significant improvement in serum aminotransferase or hepatic steatosis, and the serum low-density lipoprotein of their patients receiving

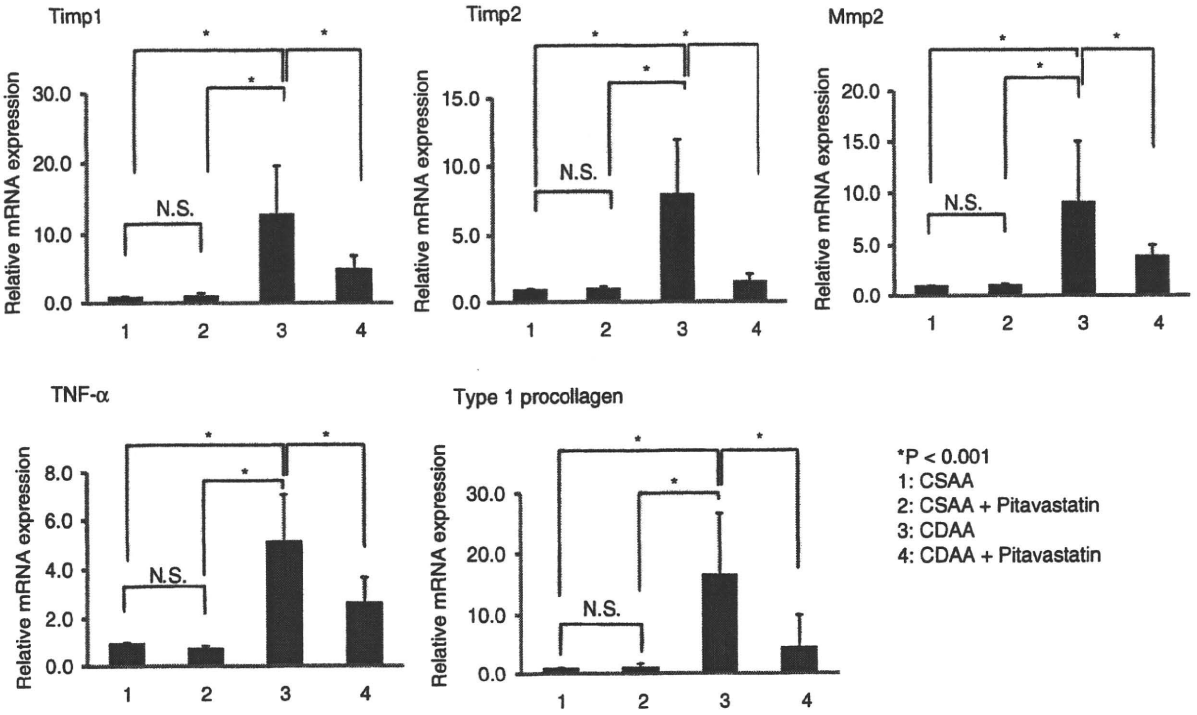

Figure 4 mRNA expressions of tissue inhibitor of metalloproteinase (TIMP)-1, TIMP-2, matrix metalloproteinase (MMP)-2, tumor necrosis factor (TNF)-α, and type I procollagen. All gene expressions increased in choline-deficient L-amino acid-defined (CDAA)-fed rats, and were significantly attenuated with pitavastatin. Pitavastatin itself had no effect on these expressions in choline-supplemented L-amino acid-defined (CSAA)-fed rats. Data are shown as the means ± standard deviations. N.S., not significant.

simvastatin treatment was not reduced significantly, so one explanation for the different results is the insufficient efficacy of statins. It has been revealed that statins reduce TG in the liver by increasing PPAR-α expression and FA β-oxidation.[12,13] In this study, the serum aminotransferase, steatosis and TG in the liver were significantly reduced by pitavastatin in CDAA-diet rats. These findings are in agreement with the results of numerous clinical and experimental studies. On the other hand, it is important to prevent secondary factors when treating NASH to inhibit liver fibrosis. In clinical trials, the efficacy of statins for liver fibrosis is controversial. Hyogo's data reported that atorvastatin did not reduce liver fibrosis in some cases,[14] whereas Ekstedt *et al.* reported that statins prevented the progression of liver fibrosis despite a high-risk profile and they recommended prescribing statins for patients with elevated liver enzymes because of NAFLD.[26] There have been no studies of the long-term effects of statins, so more clinical research, such as controlled trials, is needed.

Statins have been shown to exhibit pleiotropic effects, including anti-inflammatory, plaque-stabilizing, antithrombotic, antifibrotic and antiproliferative properties,[17,28] and they are also considered to be effective for anti-steatosis and anti-tumorigenesis. Many investigations have reported that statins inhibit fibrosis in various organs[18,29,30] but there are no reports about the efficacy of statins for fibrosis, including liver steatosis and carcinogenesis in NASH, using animal models. Although the CDAA-diet rat does not wholly reflect the human form of this disease, it is a well-established, widely recognized and accepted animal model of NASH.[9,31] At the cellular and molecular levels, liver fibrosis is mainly characterized by cellular activation of HSC and is highly associated with the expression of collagen gene expression, mediators such as TGF-β1, TNF-α, PPAR-γ and oxidative stress.[32–35] In the present experiment, nitrotyrosine was used as an indicator of oxidative stress[22] and after 10-week CDAA diets, the expressions of TGF-β1, TNF-α and oxidative stress were increased, and pitavastatin significantly reduced their expressions and then reduced TIMP-1 and -2 mRNA, which play important roles in the progression of liver fibrosis.[35]

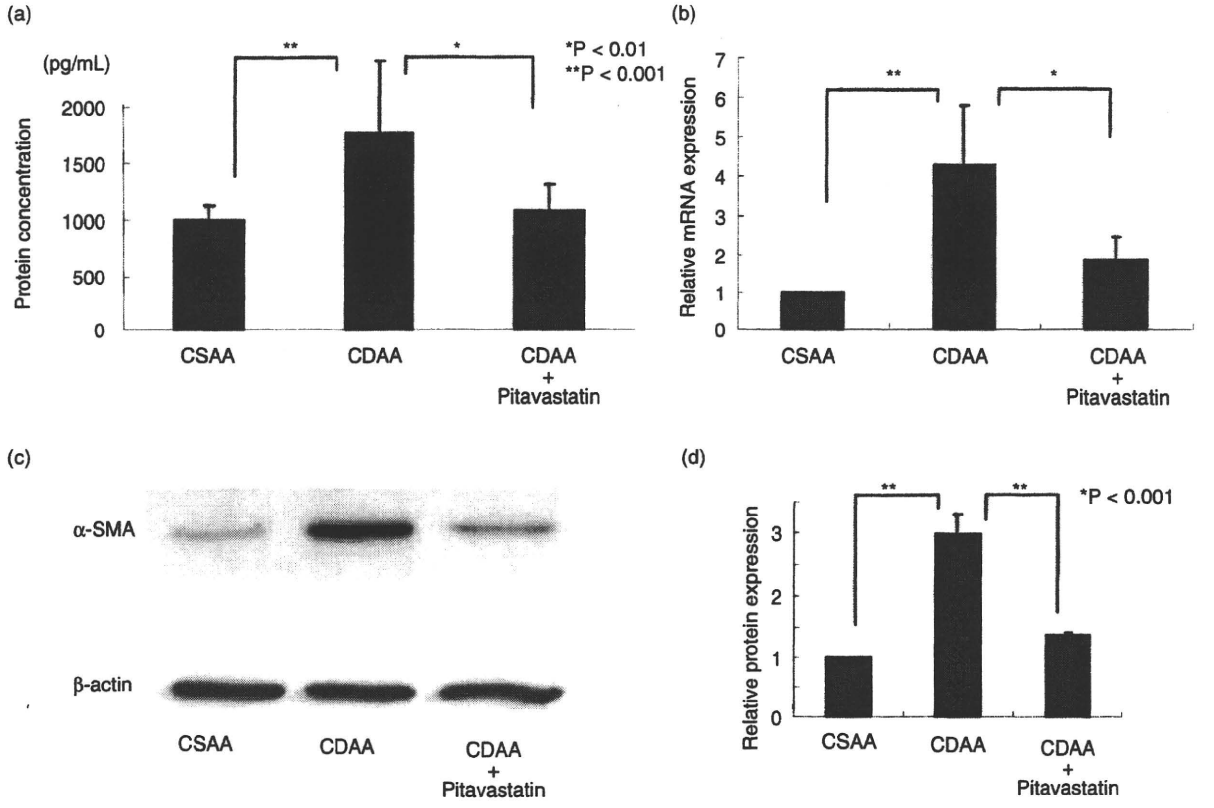

Figure 5 (a) Transforming growth factor (TGF)-β1 protein expression in serum was measured by enzyme-linked immunosorbent assay. TGF-β1 expression increased in choline-deficient L-amino acid-defined (CDAA)-fed rats, and was significantly attenuated by pitavastatin. Data are shown as the means ± standard deviations. (b) TGF-β1 mRNA expression in the liver was increased in CDAA-fed rats and significantly attenuated by pitavastatin. Data are shown as the means ± standard deviations. (c) Western blotting of α-smooth muscle actin (α-SMA) expressions in the liver of rats. (d) Quantitative analysis relative to choline-supplemented L-amino acid-defined (CSAA)-fed rats. α-SMA protein expressions increased in CDAA-fed rats, and pitavastatin administration significantly attenuated them. Data are shown as the means ± standard deviations.

Pitavastatin also inhibited the expression of MMP-2 in this study. Because MMP-2 has been reported to increase when HSC are activated,[36] MMP-2 depression may reveal the inhibition of stellate cell activation by pitavastatin. PPAR-γ is reported as the key molecule of stellate cell activity[37] and several ligands of PPAR-γ prevent the activation of stellate cells and fibrogenesis.[38,39] In this study, the expression of PPAR-γ in HSC decreased and HSC were activated after culture for several days. Pitavastatin increased PPAR-γ and prevented fibrogenesis by inhibiting the activation of HSC, like other PPAR-γ ligands.[9] In our experimental study, pitavastatin significantly improved these liver functions and reduced fibrosis in rat liver.

Because the CDAA-fed rats used in the present study are predisposed to HCC, they were also used for the study of carcinogenesis inhibition. In the present experiment, pitavastatin significantly inhibited the development of GST-P-positive lesions, a precancerous state followed by possibility of inhibiting HCC. Statins reduced the risk of several kinds of cancers[40] and the effects of statins, such as the inhibition of cell proliferation, promotion of apoptosis, and inhibition of angiogenesis and metastasis, have been reported.[41] Our data suggest that statins are capable of inhibiting carcinogenesis in NASH patients.

Thus, the present study confirmed the diverse effects of statins, such as anti-inflammatory, antifibrotic and anticarcinogenic, in a rat model of NASH; therefore, not only currently recognized therapeutic agents, such as vitamin E, thiazolidinedione and ARB, but also statins may be useful preventive agents for NASH.

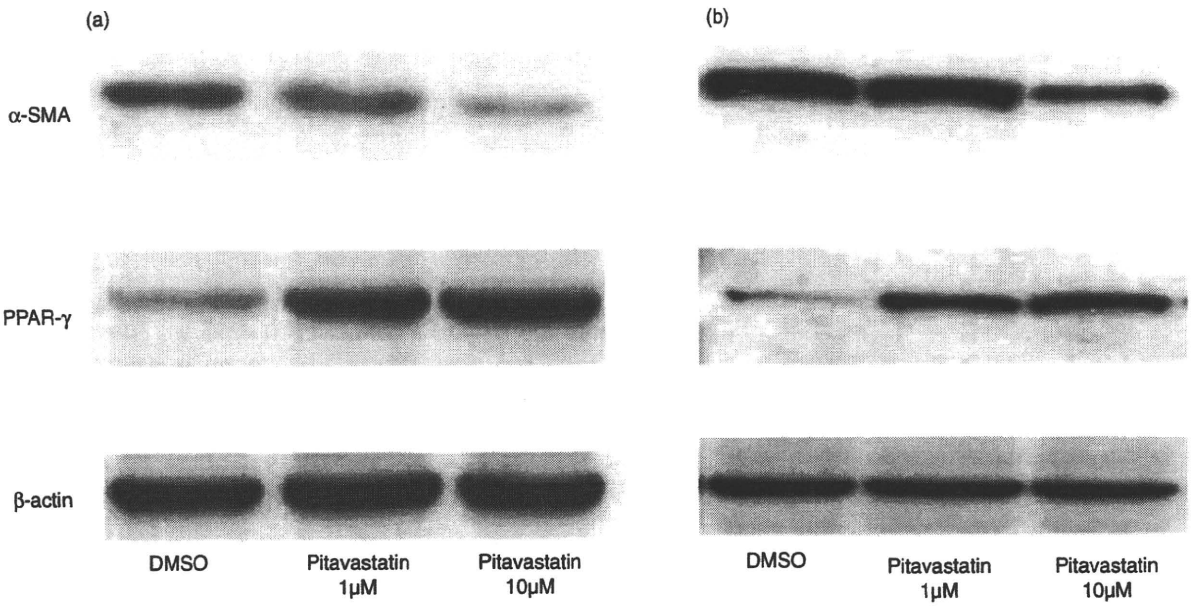

Figure 6 α-Smooth muscle actin (α-SMA) and peroxisome proliferator-activated receptor-γ (PPAR-γ) protein expression on stellate cells. (a) Human hepatic stellate cell (HSC) line LX-2 was incubated with Dulbecco's modified Eagle's medium (DMEM) for 24 h and medium with various concentrations of pitavastatin, and harvested after 24 h. (b) HSC were isolated from the rats and incubated with DMEM for 4 h, and then the culture medium was replaced with medium containing pitavastatin or the same concentration of dimethylsulfoxide (DMSO) as a control, and were harvested after 3 days. In both experiments, α-SMA decreased and PPAR-γ increased gradually after adding pitavastatin in a dose-dependent manner.

REFERENCES

1 Hashimoto E, Yatsuji S, Shiratori K *et al.* The characteristics and natural history of Japanese patients with nonalcoholic fatty liver disease. *Hepatol Res* 2005; **33**: 72–6.
2 Day CP, James OF. Steatohepatitis: a tale of two "hits"? *Gastroenterology* 1998; **114**: 842–5.
3 Yu J, Ip E, Farrell GC *et al.* COX-2 induction in mice with experimental nutritional steatohepatitis: role as pro-inflammatory mediator. *Hepatology* 2006; **43**: 826–36.
4 Sanyal AJ, Chalasani N, Robuck PR *et al.* Pioglitazone, vitamin E, or placebo for nonalcoholic steatohepatitis. *N Engl J Med* 2010; **362**: 1675–85.
5 Hirose A, Ono M, Onishi S *et al.* Angiotensin II type 1 receptor blocker inhibits fibrosis in rat nonalcoholic steatohepatitis. *Hepatology* 2007; **45**: 1375–81.
6 Yokohama S, Yoneda M, Nakamura K *et al.* Therapeutic efficacy of an angiotensin II receptor antagonist in patients with nonalcoholic steatohepatitis. *Hepatology* 2004; **40**: 1222–5.
7 Belfort R, Harrison SA, Cusi K *et al.* A placebo-controlled trial of pioglitazone in subjects with nonalcoholic steatohepatitis. *N Engl J Med* 2006; **355**: 2297–307.
8 Neuschwander-Tetri BA, Brunt EM, Wehmeier KR, Oliver D, Bacon BR. Improved nonalcoholic steatohepatitis after 48 weeks of treatment with the PPAR-gamma ligand rosiglitazone. *Hepatology* 2003; **38**: 1008–17.
9 Kawaguchi K, Sakaida I, Tsuchiya M, Omori K, Takami T, Okita K. Pioglitazone prevents hepatic steatosis, fibrosis, and enzyme-altered lesions in rat liver cirrhosis induced by a choline-deficient L-amino acid-defined diet. *Biochem Biophys Res Commun* 2004; **315**: 187–95.
10 Ratziu V, Giral P, Poynard T *et al.* Rosiglitazone for nonalcoholic steatohepatitis: one-year results of the randomized placebo-controlled Fatty Liver Improvement with Rosiglitazone Therapy (FLIRT) Trial. *Gastroenterology* 2008; **135**: 100–10.
11 Baigent C, Keech A, Simes R *et al.* Efficacy and safety of cholesterol-lowering treatment: prospective meta-analysis of data from 90,056 participants in 14 randomised trials of statins. *Lancet* 2005; **366**: 1267–78.
12 Roglans N, Sanguino E, Sanchez RM *et al.* Atorvastatin treatment induced peroxisome proliferator-activated receptor alpha expression and decreased plasma nonesterified fatty acids and liver triglyceride in fructose-fed rats. *J Pharmacol Exp Ther* 2002; **302**: 232–9.
13 Egawa T, Toda K, Onishi S *et al.* Pitavastatin ameliorates severe hepatic steatosis in aromatase-deficient (Ar−/−) mice. *Lipids* 2003; **38**: 519–23.

14 Hyogo H, Tazuma S, Chayama K *et al.* Efficacy of atorvastatin for the treatment of nonalcoholic steatohepatitis with dyslipidemia. *Metabolism* 2008; **57**: 1711–8.
15 Gomez-Dominguez E, Gisbert JP, Moreno-Monteagudo JA, Garcia-Buey L, Moreno-Otero R. A pilot study of atorvastatin treatment in dyslipemid, non-alcoholic fatty liver patients. *Aliment Pharmacol Ther* 2006; **23**: 1643–7.
16 Rallidis LS, Drakoulis CK, Parasi AS. Pravastatin in patients with nonalcoholic steatohepatitis: results of a pilot study. *Atherosclerosis* 2004; **174**: 193–6.
17 Zhou Q, Liao JK. Pleiotropic effects of statins. – Basic research and clinical perspectives. *Circ J* 2010; **74**: 818–26.
18 Yagi S, Aihara K, Matsumoto T *et al.* Pitavastatin, an HMG-CoA reductase inhibitor, exerts eNOS-independent protective actions against angiotensin II induced cardiovascular remodeling and renal insufficiency. *Circ Res* 2008; **102**: 68–76.
19 Sakaida I, Tsuchiya M, Kawaguchi K, Kimura T, Terai S, Okita K. Herbal medicine Inchin-ko-to (TJ-135) prevents liver fibrosis and enzyme-altered lesions in rat liver cirrhosis induced by a choline-deficient L-amino acid-defined diet. *J Hepatol* 2003; **38**: 762–9.
20 Anstee QM, Goldin RD. Mouse models in non-alcoholic fatty liver disease and steatohepatitis research. *Int J Exp Pathol* 2006; **87**: 1–16.
21 Kitahara A, Satoh K, Ito N *et al.* Changes in molecular forms of rat hepatic glutathione S-transferase during chemical hepatocarcinogenesis. *Cancer Res* 1984; **44**: 2698–703.
22 Umeji K, Umemoto S, Matsuzaki M *et al.* Comparative effects of pitavastatin and probucol on oxidative stress, Cu/Zn superoxide dismutase, PPAR-gamma, and aortic stiffness in hypercholesterolemia. *Am J Physiol Heart Circ Physiol* 2006; **291**: H2522–32.
23 Xu L, Friedman SL, Eng FJ *et al.* Human hepatic stellate cell lines, LX-1 and LX-2: new tools for analysis of hepatic fibrosis. *Gut* 2005; **54**: 142–51.
24 Kayano K, Sakaida I, Uchida K, Okita K. Inhibitory effects of the herbal medicine Sho-saiko-to (TJ-9) on cell proliferation and procollagen gene expressions in cultured rat HSC. *J Hepatol* 1998; **29**: 642–9.
25 Georgescu EF, Georgescu M. Therapeutic options in non-alcoholic steatohepatitis (NASH). Are all agents alike? Results of a preliminary study. *J Gastrointestin Liver Dis* 2007; **16**: 39–46.
26 Ekstedt M, Franzen LE, Mathiesen UL, Holmqvist M, Bodemar G, Kechagias S. Statins in non-alcoholic fatty liver disease and chronically elevated liver enzymes: a histopathological follow-up study. *J Hepatol* 2007; **47**: 135–41.
27 Nelson A, Torres DM, Morgan AE, Fincke C, Harrison SA. A pilot study using simvastatin in the treatment of nonalcoholic steatohepatitis: a randomized placebo-controlled trial. *J Clin Gastroenterol* 2009; **43**: 990–4.
28 Davignon J, Laaksonen R. Low-density lipoprotein-independent effects of statins. *Curr Opin Lipidol* 1999; **10**: 543–59.
29 Shishehbor MH, Brennan ML, Hazen SL *et al.* Statins promote potent systemic antioxidant effects through specific inflammatory pathways. *Circulation* 2003; **108**: 426–31.
30 Goppelt-Struebe M, Hahn A, Iwanciw D, Rehm M, Banas B. Regulation of connective tissue growth factor (ccn2; ctgf) gene expression in human mesangial cells: modulation by HMG CoA reductase inhibitors (statins). *Mol Pathol* 2001; **54**: 176–9.
31 Sakaida I, Hironaka K, Uchida K, Suzuki C, Kayano K, Okita K. Fibrosis accelerates the development of enzyme-altered lesions in the rat liver. *Hepatology* 1998; **28**: 1247–52.
32 Nieto N, Friedman SL, Greenwel P, Cederbaum AI. CYP2E1-mediated oxidative stress induces collagen type I expression in rat HSC. *Hepatology* 1999; **30**: 987–96.
33 Gressner AM, Weiskirchen R. Modern pathogenetic concepts of liver fibrosis suggest stellate cells and TGF-beta as major players and therapeutic targets. *J Cell Mol Med* 2006; **10**: 76–99.
34 Pinzani M, Rombouts K. Liver fibrosis: from the bench to clinical targets. *Dig Liver Dis* 2004; **36**: 231–42.
35 Tomita K, Tamiya G, Hibi T *et al.* Tumour necrosis factor alpha signalling through activation of Kupffer cells plays an essential role in liver fibrosis of non-alcoholic steatohepatitis in mice. *Gut* 2006; **55**: 415–24.
36 Benyon RC, Iredale JP, Goddard S, Winwood PJ, Arthur MJ. Expression of tissue inhibitor of metalloproteinases 1 and 2 is increased in fibrotic human liver. *Gastroenterology* 1996; **110**: 821–31.
37 Tsukamoto H. Fat paradox in liver disease. *Keio J Med* 2005; **54**: 190–2.
38 Galli A, Crabb DW, Casini A *et al.* Antidiabetic thiazolidinediones inhibit collagen synthesis and hepatic stellate cell activation in vivo and in vitro. *Gastroenterology* 2002; **122**: 1924–40.
39 Miyahara T, Schrum L, Tsukamoto H *et al.* Peroxisome proliferator-activated receptors and hepatic stellate cell activation. *J Biol Chem* 2000; **275**: 35715–22.
40 Demierre MF, Higgins PD, Gruber SB, Hawk E, Lippman SM. Statins and cancer prevention. *Nat Rev Cancer* 2005; **5**: 930–42.
41 Gauthaman K, Fong CY, Bongso A. Statins, stem cells, and cancer. *J Cell Biochem* 2009; **106**: 975–83.

The American Journal of Pathology, Vol. 177, No. 2, August 2010

DOI: 10.2353/ajpath.2010.090430

Hepatic Hyperplasia Associated with Discordant Xenogeneic Parenchymal-Nonparenchymal Interactions in Human Hepatocyte-Repopulated Mice

Rie Utoh,*† Chise Tateno,*‡§ Miho Kataoka,* Asato Tachibana,*§ Norio Masumoto,*¶ Chihiro Yamasaki,*§ Takashi Shimada,§ Toshiyuki Itamoto,¶ Toshimasa Asahara,¶ and Katsutoshi Yoshizato*‡§‖**

From the Yoshizato Project, Cooperative Link of Unique Science and Technology for Economy Revitalization (CLUSTER), Hiroshima Prefectural Institute of Industrial Science and Technology, Hiroshima; the Institute of Advanced Biomedical Engineering and Science,† Tokyo Women's Medical University, Tokyo; the Hiroshima University Liver Project Research Center,‡ Hiroshima; PhoenixBio Co.,§ Hiroshima; the Department of Surgery,¶ Division of Frontier Medical Science, Graduate School of Biomedical Sciences, Hiroshima University, Hiroshima; Liver Research Center, Osaka City University Graduate School of Medicine, Osaka; and the Department of Biological Science,** Developmental Biology Laboratory and Hiroshima University 21st Century COE Program for Advanced Radiation Casualty Medicine, Graduate School of Science, Hiroshima University, Hiroshima, Japan*

Liver mass is optimized in relation to body mass. Rat (r) and human (h) hepatocytes were transplanted into liver-injured immunodeficient mice and allowed to proliferate for 3 or 11 weeks, respectively, when the transplants stopped proliferating. Liver/body weight ratio was normal throughout in r-hepatocyte-bearing mice (r-hep-mice), but increased continuously in h-hepatocyte-bearing mice (h-hep-mice), until reaching approximately three times the normal m-liver size, which was considered to be hyperplasia of h-hepatocytes because there were no significant differences in cell size among host (mouse [m-]) and donor (r- and h-) hepatocytes. Transforming growth factor-β (TGF-β) type I receptor, TGF-β type II receptor, and activin A type IIA receptor mRNAs in proliferating r-hepatocytes of r-hep-mice were lower than in resting r-hepatocytes (normal levels) and increased to normal levels during the termination phase. Concomitantly, m-hepatic stellate cells began to express TGF-β proteins. In stark contrast, TGF-β type II receptor and activin A type IIA receptor mRNAs in h-hepatocytes remained low throughout and m-hepatic stellate cells did not express TGF-β in h-hep-mice. As expected, Smad2 and 3 translocated into nuclei in r-hep-mice but not in h-hep-mice. Histological analysis showed a paucity of m-stellate cells in h-hepatocyte colonies of h-hep-mouse liver. We conclude that m-stellate cells are able to normally interact with concordant r-hepatocytes but not with discordant h-hepatocytes, which seems to be at least partly responsible for the failure of the liver size optimization in h-hep-mice. ***(Am J Pathol 2010, 177:000–000; DOI: 10.2353/ajpath.2010.090430)***

Experiments using animal models with damaged livers have demonstrated the high replicative potential of hepatocytes. A transgenic (Tg) mouse carrying an albumin (Alb) enhancer/promoter-driven murine urokinase-type plasminogen activator (uPA) gene was created[1]; the liver of this mouse degenerates and increases hepatocyte growth factor production and induces the proliferation of normal hepatocytes.[2] When transplanted into the uPA-Tg mice, mouse (m) hepatocytes engrafted into the host liver and proliferated, eventually replacing the host hepatocytes with a replacement index (RI) of 80%,[3] where RI represents the ratio of the regions occupied by transplanted hepatocytes in the host liver). The offspring generated by crossing uPA-Tg mice with immunodeficient mice were used as hosts for the xenotransplantation of rat (r),[4] woodchuck,[5] and human (h) hepatocytes.[6–8]

We showed that the repopulation kinetics of r-hepatocytes in uPA/severe combined immunodeficiency (SCID) mice were different from those of h-hepatocytes.[9] Rat hepatocytes rapidly proliferated and completely repopulated the mouse liver, whereas h-hepatocytes proliferated slowly over a longer period, with RI = ~90%. However,

Supported in part by Cooperative Link of Unique Science and Technology for Economy Revitalization (CLUSTER), Promotion of Science and Technology in Regional Areas, Ministry of Education, Culture, Sports, Science and Technology, Japan.

Accepted for publication March 30, 2010.

None of the authors declare any relevant financial relationships.

Address reprint requests to Katsutoshi Yoshizato, Ph.D., PhoenixBio Co., Ltd., 3-4-1 Kagamiyama, Higashihiroshima, Hiroshima 739-0046, Japan. E-mail: katsutoshi.yoshizato@phoenixbio.co.jp.

the livers of mice bearing h-hepatocytes (h-hep-mice) became much larger than the normal mass of the host mouse liver as the RI increased, whereas their counterparts with r-hepatocytes (r-hep-mice) did not (unpublished data). The above result with h-hep-mice does not meet the empirical rule (liver size optimization rule) that liver size is determined by the size of an animal's body.[10] This rule says that livers from smaller animals transplanted to larger animals must increase in size, which has been demonstrated in dogs,[10] humans,[11] and rats.[12]

Transforming growth factor (TGF)-β[13,14] and activin[15] are potent inhibitors of hepatocyte proliferation. The initiation of TGF-β signaling requires binding to the TGF-β type II receptor (TGFBR2), a constitutively active serine-threonine kinase, which subsequently *trans*-phosphorylates TGF-β type I receptor (TGFBR1). Activated TGFBR1 phosphorylates the Smad family proteins, Smad2 and 3 (Smad2/3), which then complex with Smad4 and translocate into the nucleus.[16] Smad2/3 are also activated by activin and nodal receptors, members of the TGF-β superfamily.[17] After partial hepatectomy, TGF-β mRNA expression increased in nonparenchymal cells, and TGF-β seemed to function as an inhibitory paracrine factor to prevent uncontrolled hepatocyte growth.[18]

When hepatocyte-targeted TGFBR2-knockout (KO) mice were subjected to 70% partial hepatectomy, hepatocytes grew beyond the limit of the known liver/body weight ratio ($R_{L/B}$),[19] supporting the antiproliferative role of TGF-β signaling. However, a similar study with hepatocyte-targeted TGFBR2-KO mice showed no significant differences in $R_{L/B}$ between control and KO mice because of an alternative increase in signaling via activin A/activin A type IIA receptor (ACVR2A) and persistent Smad pathway activity.[20] Thus, the roles of TGF-β, activin, and their receptors in the regulation of liver mass remain to be further studied.

In the present study, we compared the repopulation processes of concordant (rat) and discordant (human) xenogeneic hepatocytes in the uPA/SCID mouse liver. Our results showed that r-hep-mice had normal mouse regulation of $R_{L/B}$, whereas h-hep-mice underwent liver hyperplasia, resulting in the increase in $R_{L/B}$. The present study strongly suggests that discordant h-hepatocytes fail in exchanging molecular signals including TGF-β/activin with m-hepatic stellate cell (HSCs) and proliferate over the liver size optimization rule for mouse.

Materials and Methods

Preparation of Liver Tissues and Hepatocytes

The Hiroshima Prefectural Institute of Industrial Science and Technology Ethics Board approved this study. Liver tissues were obtained from seven donors in hospitals, with informed consent before the operations in accordance with the 1975 Declaration of Helsinki: four males, a 12-year-old male (12YM), a 28-year-old male (28YM), a 49-year-old male (49YM), and a 50-year-old male (50YM), and three females, a 25-year-old female (25YF), a 61-year-old female (61YF), and a 65-year-old female (65YF). The livers from the 25YF, 28YM, and 61YF were used for real-time RT-PCR to determine the expression levels of cell cycle-related genes and TGFBR/ACVR genes, and those from the 49YM, 50YM, and 65YF were used for immunostaining of proteins. Liver tissues were resected from 13-week-old male Fischer 344 rats (Charles River, Yokohama, Japan) and were used for real-time RT-PCR to determine the expression levels and immunohistochemistry.

h-Hepatocytes were isolated from the 12YM as reported previously.[7,21] Cryopreserved h-hepatocytes from two males, a 9-month-old male (9MM) and a 13-year-old male (13YM), were obtained from In Vitro Technologies (Baltimore, MD); h-hepatocytes from a 10-year-old female (10YF) were purchased from BD Biosciences (San Jose, CA). The hepatocytes from these four donors were used for transplantation experiments into uPA/SCID mice. r-Hepatocytes were isolated from the livers of Fischer 344 rats by collagenase perfusion,[22] centrifuged through 45% Percoll at 50 $\times$ *g* for 24 minutes and used for transplantation experiments. These hepatocyte preparations all showed >80% of viability, which was determined by the dye extrusion test, and >99% of purity, which was determined by microscopic observation.

Transplantation of Hepatocytes

h- and r-Hepatocytes, 7.5×10^5 and 5×10^5 cells, respectively, were transplanted into the liver of homozygous uPA/SCID mice, which had been generated by crossing uPA-Tg mice with SCID mice.[7] Donor h-hepatocytes showed reproducibly high engraftment efficiency similar to fresh r-hepatocytes and RI >80% under the optimized conditions. The labeling index (LI) of 5-bromo-2′-deoxyuridine (BrdU) of the transplanted hepatocytes was determined as a measure of DNA synthesis by exposing the host animals to BrdU for 1 hour before sacrifice.[23]

Histochemistry

Paraffin and frozen sections of 5-μm thickness were prepared from liver tissues as detailed previously.[7,23] The sections were stained with H&E or subjected to immunohistochemical analysis using the primary antibodies listed in Table 1 together with necessary information. For bright-field immunohistochemistry, the antibodies were visualized with the VECTASTAIN ABC kit (Vector Laboratories, Burlingame, CA) using 3,3′-diaminobenzidine as the substrate. The sections were counterstained with Mayer's hematoxylin. Fluorescent immunohistochemistry was performed using Alexa 488- or 594-conjugated donkey anti-mouse IgG or donkey anti-rabbit IgG (Invitrogen) as secondary antibodies and then with Hoechst 33258 for nuclear staining. Human cytokeratin 8/18 (hCK8/18) antibodies reacted with h-hepatocytes but not with m-hepatocytes. Rat major histocompatability complex class I RT1A (rRT1A) antibodies reacted with r-hepatocytes but not with m-hepatocytes. The RIs of h- and r-hepatocytes ($RI_{h\text{-}hep}$ and $RI_{r\text{-}hep}$, respectively) were calculated as the ratios of the area occupied by $hCK8/18^+$ h-hepatocytes and the area occupied by $rRT1A^+$ r-hepatocytes to the entire area ex-

Table 1. Antibodies for Immunohistochemical Analysis

Antibodies	Clone (clone name)	Host	Dilution	Fixation	Sections	Supplier
Human CK8/18*	Monoclonal (NCL 5D3)	Mouse	50	Aceton	Frozen	MP Biomedicals (Aurora, OH)
Human albumin* (cross-adsorbed)	Polyclonal	Goat	200	Formalin	Paraffin	Bethyl Laboratories (Montgomery, TX)
BrdU	Monoclonal (Bu20a)	Mouse	50	Formalin	Paraffin	DAKO (Glostrup, Denmark)
Rat RT1A†	Monoclonal (OX-18)	Mouse	100	Aceton	Frozen	Chemicon International (Temecula, CA)
Mouse type IV collagen	Polyclonal	Rabbit	500	Aceton	Frozen	LSL (Tokyo, Japan)
Human MRP2‡	Polyclonal	Rabbit	200	Aceton	Frozen	Sigma (St. Louis, MO)
Human TGFBR2§	Polyclonal	Rabbit	500	Aceton	Frozen	Upstate (Billerica, MA)
TGF-β1¶	Polyclonal	Rabbit	10	Formalin	Frozen	BioVision (Mountain View, CA)
Human desmin§	Monoclonal	Mouse	50	Formalin	Frozen	DAKO
Human Smad2§	Polyclonal	Rabbit	50	Non-fixed	Frozen	Zymed Laboratories (South San Francisco, CA)
Human Smad3§	Polyclonal	Rabbit	200	Formalin	Paraffin	Zymed Laboratories
Human E-cadherin§	Polyclonal	Rabbit	200	Formalin	Frozen	Abcam (Cambridge, MA)

*Human-specific antibody.
†Rat-specific antibody.
‡Cross-reactive with rat antigen.
§Cross-reactive with rat and mouse antigens.
¶Cross-reactive with TGF-β1-3.

amined on immunohistochemical sections from six lobes, respectively, as described previously.[7] BrdU LIs of h- and r-hepatocytes ($LI_{h\text{-}hep}$ and $LI_{r\text{-}hep}$, respectively) were calculated as the ratios of $BrdU^+$ nuclei to $hAlb^+$ h-hepatocytes and $rRT1A^+$ r-hepatocytes, respectively, in 10 randomly selected fields from three different lobes.

A transferase-mediated dUTP nick end-labeling (TUNEL) assay was performed as follows. Paraffin-embedded liver tissues were sectioned, deparaffinized, and subjected to TUNEL analysis using an ApopTag Peroxidase In Situ Apoptosis Detection Kit (Chemicon International, Temecula, CA) following the manufacturer's instructions.

Real-Time RT-PCR

Total RNA was isolated from normal and chimeric liver tissues using Isogen (Nippon Gene, Tokyo, Japan) and aliquots, 1 μg each, were reverse-transcribed with random hexamers using PowerScript Reverse Transcriptase (Clontech, Kyoto, Japan). The expressions of the following genes were measured by real-time RT-PCR using an SYBR Green PCR Master Mix (Applied Biosystems, Foster City, CA) in an ABI Prism 7700 sequence detector (Applied Biosystems): h-forkhead box M1 (hFoxM1), h-cyclin dependent kinases (hCdk) 1, hCyclin B1, hCyclin D1, h-cell division cycle 25A (hCdc25A), hTGFBR1, hTGFBR2, hACVR2A, h-glyceraldehyde 3-phosphate dehydrogenase (hGAPDH), rat TGFBR1 (rTGFBR1), rTGFBR2, rACVR2A, and rGAPDH. The gene-specific primers we used are shown in Table 2. These primers correctly amplified the corresponding human/rat genes but not the mouse genes. The relative mRNA expressions of transplanted h- and r-hepatocytes were quantified using the comparative threshold cycle ($\Delta\Delta C_t$) method[24] according to the manual provided by Applied Biosystems. hGAPDH and rGAPDH, respectively, were used as the internal reference genes to normalize the expression of human/rat target genes; h/r-specific primers were used because there is a difference in the amounts of h/r-cDNAs in the

Table 2. Primer Sets for Real-Time RT-PCR

Gene	Forward primer	Reverse primer
hFoxM1	5′-GCATCTACTGCCTCCCTGTG-3′	5′-GAGGAGTCTGCTGGGAACG-3′
hCdk1	5′-AAACTACAGGTCAAGTGG-3′	5′-GGGATAGAATCCAAGTATTTCTTCAG-3′
hCyclin B1	5′-CCTGATGGAACTAACTATGTTG-3′	5′-CATGTGCTTTGTAAGTCCTTGA-3′
hCyclin D1	5′-TGTGAAGTTCATTTCCAATCCG-3′	5′-CTGGAGAGGAAGCGTGTGAG-3′
hCdc25A	5′-CAAAGAGGAGGAAGAGCATGTC-3′	5′-CCAGGGATAAAGACTGATGAAGAG-3′
hTGFBR1	5′-GGAATTCATGAAGATTACCAAC-3′	5′-AGAGTTCAGGCAAAGCTGTAGA-3′
hTGFBR2	5′-CATGTGTTCCTGTAGCTCTGAT-3′	5′-TGCCGGTTTCCCAGGTTGA-3′
hACVR2A	5′-AAGAAGACCCTTTGTTGAAAAATG-3′	5′-GCAAGGTTTCTCTTAGTCTCATGTC-3′
hSmad2	5′-AAAGCTTCACCAATCAAGTCC-3′	5′-CTTCTCTTCCTCTTTAATGGG-3′
hSmad3	5′-TGGAACTCTACTCAACCCAT-3′	5′-GGTAAATGTGTTTGGCAGAC-3′
hGAPDH	5′-ACCAGGGCTGCTTTTAACTC-3′	5′-ATTGATGACAAGCTTCCCG-3′
rTGFBR1	5′-CACTTCTGATTCCCACTCTTG-3′	5′-ATGAAGGAGCAGGAGCTGTA-3′
rTGFBR2	5′-CAAGTCGGTTAACAGCGAT-3′	5′-GGCTTCTCACAGATGGAGG-3′
rACVR2A	5′-AGCATGGATTGGGAGACTTC-3′	5′-GCCACATTCTTCGTGTAAGTT-3′
rGAPDH	5′-CCAGGGCTGCCTTCTCTTGTGA-3′	5′-GCCGTTGAACTTGCCGTGGGTA-3′

h, human-specific; r, rat-specific.

mixed baths from the h- or r-hep-mouse liver. Before performing quantification with the $\Delta\Delta C_T$ method, we confirmed that the amplification efficiencies of target and reference primers were approximately equal. The expression levels of the target genes show the relative differences from the normal h/r-liver controls. For all data, the h/r target C_T value was normalized using the formula: $\Delta C_T = C_T$ h/r target $- C_T$ h/rGAPDH. To determine the relative expression levels, the formula, $\Delta\Delta C_T = \Delta C_T$ sample (chimeric livers) $- \Delta C_T$ calibrator (h/r-livers), was used and $2^{-\Delta\Delta C_T}$ was plotted.

Statistics

Results are shown as the mean ± SD. Significant differences between groups were detected with Dunnett's multiple comparison test or Student's *t*-tests using StatView software (SAS Institute Japan, Tokyo, Japan).

Results

Growth Kinetics for r- and h-Hepatocytes in uPA/SCID Mice

Twelve mice were transplanted with r-hepatocytes and sacrificed at 1, 2, 3, and 4 weeks after transplantation. Liver sections were subjected to double immunostaining for BrdU and rRT1A to determine the $LI_{r\text{-}hep}$ and the $RI_{r\text{-}hep}$ (Figure 1A), where $LI_{r\text{-}hep}$ represents the ratio of the BrdU-positive r-hepatocyte number to the total r-hepatocytes in the r-hepatocyte-repopulated region in the r-hep-mouse liver, and $RI_{r\text{-}hep}$ represents the ratio of the repopulated r-hepatocytes to the total r- and m-hepatocytes in the r-hep-mouse liver. $LI_{r\text{-}hep}$ was approximately 15% at 1 week, when $RI_{r\text{-}hep}$ was approximately 7%. $RI_{r\text{-}hep}$ reached almost 100% at 3 weeks when $LI_{r\text{-}hep}$ had markedly decreased to 1%. Finally, $LI_{r\text{-}hep}$ returned to the control level (0.4%) at 4 weeks, the level of LI of SCID mouse liver. From these results, we concluded that r-hepatocytes terminated proliferation at approximately 3 weeks.

Mice were transplanted with h-hepatocytes isolated from the 9MM ($h\text{-}hep_{9MM}$) and were sacrificed at 1 to 11 weeks after transplantation (Figure 1B). $LI_{h\text{-}hep}$ and $RI_{h\text{-}hep}$, the corresponding ratios for h-hep-mouse liver, were approximately 10% and <1% at 1 week, respectively. The $LI_{h\text{-}hep}$ at this time period was 64% of the $LI_{r\text{-}hep}$. The rise of $RI_{h\text{-}hep}$ and the decrease of $LI_{h\text{-}hep}$ thereafter were both greatly slow compared with those of the r-hep-mice. $LI_{h\text{-}hep}$ returned to the control level at 11 weeks when $RI_{h\text{-}hep}$ was still as low as 58 ± 46%. Thus, it was concluded that h-hepatocytes repopulate the m-liver quite slowly. We believe that this difference in donor proliferative and repopulating activities is due to species-related differences but not experimental variables that might influence transplantation outcomes, because, first, the engraftment efficiencies were similar between the h- and the r-hepatocytes, second, the viability (>80%) and the purity (>99%) of the hepatocyte preparations were comparable between the two types of hepatocytes, and, third, the similar difference was observed in the previous report in which h-hepatocytes were also used as donor hepatocytes.[9]

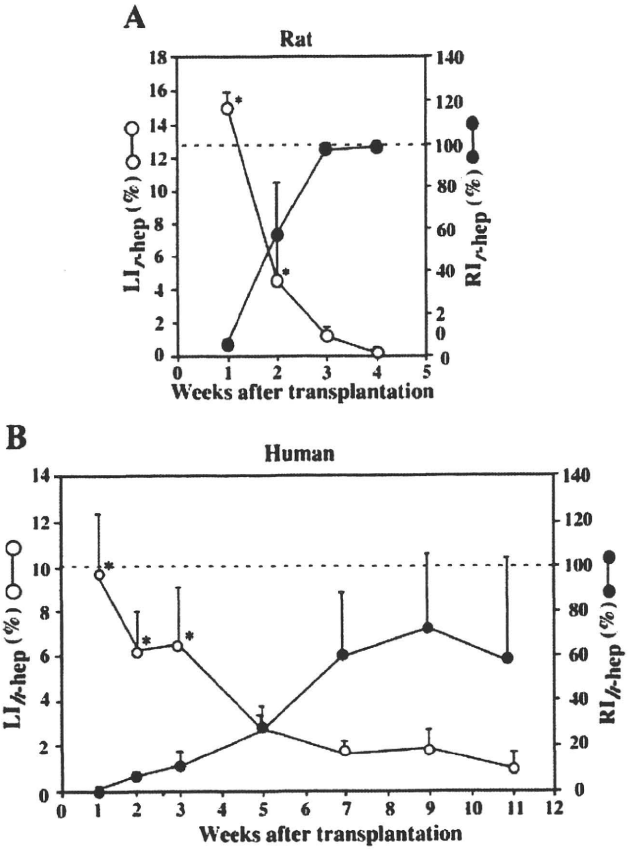

Figure 1. Repopulation of r- and h-hepatocytes in mice. uPA/SCID mice were transplanted with r-hepatocytes (**A**) and h-hepatocytes (**B**) and sacrificed at the indicated times (weeks) after transplantation. **A:** r-hep-Mice. Histological sections were prepared from three different lobes and stained for rRT1A and BrdU. $rRT1A^+$ and $BrdU^+$ double-positive hepatocytes and $rRT1A^-$ hepatocytes were counted to determine $LI_{r\text{-}hep}$ (open circle) and $RI_{r\text{-}hep}$ (closed circle), respectively. **B:** $h\text{-}hep_{9MM}$-Mice. $LI_{h\text{-}hep}$ (open circle) and $RI_{h\text{-}hep}$ (closed circle) were similarly determined, except that h-hepatocytes were identified using hAlb antibodies. The LI of livers taken from control animals (8- to 15-week-old SCID mice) was 0.4 ± 0.2% (n = 3). Significant differences compared with normal livers (*$P < 0.05$). The dotted horizontal line indicates RI = 100%.

Information regarding proliferative activity of h-hepatocytes was obtained by determining the gene expression levels of five cell cycle promotion genes (hCdk1, hCyclin B, hFoxM1, hCdc25A, and hCyclin D) in the h-hep-mouse livers during repopulation, together with those in normal h-livers from three donors. The results are shown as the relative mRNA expression levels against those in the normal h-livers (Figure 2). h-hep-Mouse livers expressed hCdk1 and hCyclin B1 at much and moderately higher levels at 3 to 9 weeks, respectively. The expressions of hFoxM1 and hCdc25A were significantly higher in h-hep-mouse livers up to 7 weeks. These genes all reduced the expression to levels comparative to normal h-liver levels at 11 weeks. These results indicate that h-hepatocytes in h-hep-mice terminated growth at 11 weeks after transplantation.

Correlation of $R_{L/B}$ with RI in h-Chimeric Mice

In the experiments shown in Figure 1, we noticed that the h-hep-mouse liver enlarged beyond the normal volume of the host liver as $RI_{h\text{-}hep}$ increased. We assessed a cor-

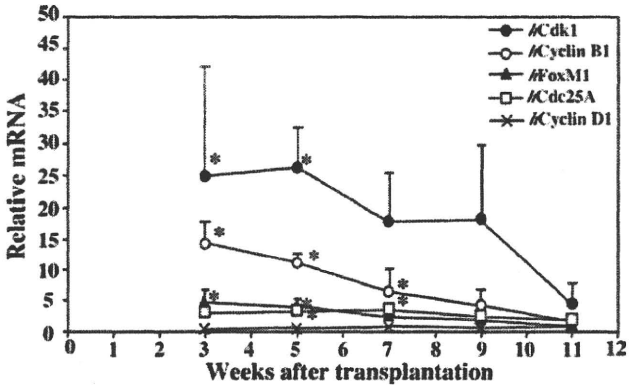

Figure 2. Expressions of cell cycle-related genes during h-hepatocyte repopulation in h-hep-mice. h-hep-Mouse livers were removed at 3 to 11 weeks after transplantation from h-hep-mice shown in Figure 1B and subjected to real-time RT-PCR for hCdk1 (closed circle), hCyclin B1 (open circle), hFoxM1 (closed triangle), hCdc25A (open square), and hCyclin D1 (×). Gene expressions were also determined for normal human livers from the 25YF, 28YM, and 61YF donors. Gene expressions were all normalized to hGAPDH expression. The ratio of mRNA expression for each gene in h-hep-mouse livers was calculated by dividing the normalized value of each gene of h-hep-mouse livers by the normalized value of corresponding gene of the normal h-livers. The ratios are plotted against weeks after transplantation. The variation of each gene of the normal livers was 1.0 ± 0.3, 1.0 ± 0.6, 1.0 ± 0.4, 1.0 ± 0.5, and 1.0 ± 0.3 for hFoxM1, hCdk1, hCyclin B1, hCyclin D1, and hCdc25A, respectively. Significant differences against normal h-livers (*$P < 0.05$).

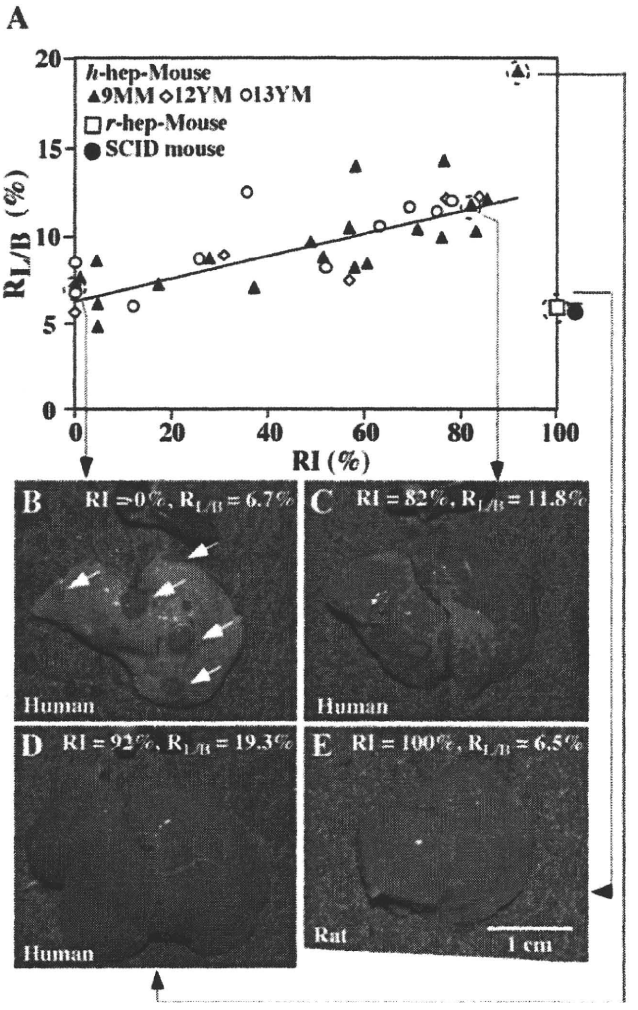

Figure 3. Correlation of $R_{L/B}$ with RI in h-hep-mice. **A:** Twenty-one, 6, and 11 h-hep-mice were produced by transplanting hepatocytes from the 9MM, 12YM, and 13YM donors, respectively, and then sacrificed at 11 to 14 weeks after transplantation. $R_{L/B}$ and RI were determined at sacrifice and plotted together. Closed triangle, 9MM hepatocytes; open diamond, 12YM hepatocytes; open circle, 13YM hepatocytes. Four r-hep-mice were produced and sacrificed at five weeks after transplantation when the repopulation had completed, and $R_{L/B}$ and RI were determined (open square). $R_{L/B}$ was also determined for three 8- to 15-week-old SCID mice (closed circle). **B–D:** Gross appearances of h-hep-mouse livers at 11 weeks. The four **long arrows** in the figure starting from each of mouse symbols in **A** point to the photos of the corresponding mouse livers shown in **B**, **C**, **D**, and **E**, respectively. **B:** The liver of an h-hep$_{9MM}$ mouse with RI = 0% and $R_{L/B}$ = 6.7%. **Arrows** indicate reddish colonies of m-hepatocytes that deleted the transgene. Whitish regions are occupied by Tg host hepatocytes. The dark red-colored organ placed above the liver is spleen removed from the same recipient. **C:** The liver of an h-hep$_{9MM}$ mouse with RI = 82% and $R_{L/B}$ = 11.8%. **D:** The liver of an h-hep$_{9MM}$ mouse with RI = 92% and $R_{L/B}$ = 19.3%. **E:** The liver of an r-hep-mouse with RI = 100% and $R_{L/B}$ = 6.5%. Scale bar = 1 cm.

relation between $RI_{h\text{-}hep}$ and liver mass during h-hepatocyte repopulation. A total of 38 h-hep-mice were generated using h-hepatocytes from three donors (9MM, 12YM, and 13YM) and were sacrificed at 11 to 14 weeks after transplantation. No significant increase in blood hAlb levels was observed at 9 to 10 weeks, indicating that the livers then had entered the termination phase of growth, which is consistent with the results shown in Figure 2. Host liver and body weights were measured at sacrifice to calculate $R_{L/B}$. Liver sections were prepared from each mouse and stained for hCK8/18 to determine RI. $R_{L/B}$ was then plotted against RI (Figure 3A). $R_{L/B}$ increased as RI increased, with a correlation coefficient (r^2) of 0.59. The gross appearances of the selected h-hep-mouse livers are shown in Figure 3, B–D. Livers of an h-hep-mouse with RI = 0% showed $R_{L/B}$ = 6.9 ± 1.0% (Figure 3, A and B). Twenty of the 38 h-hep-mice showed RI >50%. Five h-hep-mice showed RIs >80%, one of which had $R_{L/B}$ = 11.8% and is shown in Figure 3C. The highest RI was 92.1%, which was obtained in a chimeric h-hep$_{9MM}$ mouse with $R_{L/B}$ = 19.3% (Figure 3D). The $R_{L/B}$ for the five mice with RIs >80% was 13.2 ± 3.5%, which was >2-fold of the value at the time of transplantation (6.0 ± 1.1%, n = 4) or that (5.4 ± 0.5%, n = 3) observed in SCID mice (Figure 3A). Importantly, the $R_{L/B}$ of r-hep-mice did not change during repopulation (Figure 3E, 5 weeks) and was similar to that of SCID mice (5.4 ± 0.5%, n = 3): $R_{L/B}$ = 6.5 ± 1.1, 6.3 ± 0.2, 6.4 ± 0.2, and 5.8 ± 0.2% (each n = 3), at 2, 3, 4, and 5 weeks after transplantation, when RIs were 57.1 ± 24.7, 97.1 ± 3.0, 98.6 ± 2.4, and 100 ± 0.0%, respectively. This fact suggests that the increase in r-hepatocyte number and the death of injured m-hepatocytes are normally balanced in the r-hep-mouse liver. However, $R_{L/B}$ of h-hep-mice increased as the RI increased as above, suggesting a possible imbalance between h-hepatocyte proliferation and m-hepatocyte death.

To test this possibility we performed the TUNEL analysis and determined the ratios (%) of the TUNEL$^+$ (dead) m-hepatocytes during the repopulation of h-hepatocytes as follows: 0.5 ± 0.1, 0.6 ± 0.2, 1.2 ± 0.1, 0.6 ± 0.3, 0.2 ± 0.1, 3.9 ± 4.7, and 8.5 ± 6.8 at 1, 2, 3, 5, 7, 9, and 11 weeks (each n = 3), respectively. The ratios were quite low until 7 weeks after transplantation and were much lower than those of the BrdU$^+$ h-hepatocytes shown in Figure 1B (~10% at 1 week and ~2% at 7 weeks). Similar TUNEL analysis showed a TUNEL$^+$ ratio of 18.8 ± 6.1% (n = 3) for r-hep-mice at 3 weeks after transplantation, which is con-